

Ab initio molecular-dynamics study of structural, dynamical, and electronic properties of liquid Ge

Noboru Takeuchi and Ignacio L. Garzón

*Instituto de Física, Universidad Nacional Autónoma de México, Apartado Postal 2681,
22800 Ensenada, Baja California, Mexico*

(Received 14 March 1994)

We present results of a first-principles molecular-dynamics study of structural, dynamical, and electronic properties of liquid Ge. In agreement with experiments, the electronic density of states shows that liquid Ge is metallic. However, an analysis of the electronic charge density, pair correlation function, and structure factor shows the existence of some covalent bonds in the liquid. These bonds give rise to broad bands in the power spectrum, reminiscent of the vibrational modes of crystalline Ge. They are also responsible for the low coordination number found in the melt. The calculated diffusion coefficient is also in agreement with available experimental results.

I. INTRODUCTION

The liquid state of Ge, with higher density than the crystalline phase, is characterized by a metallic behavior.^{1,2} This semiconductor-to-metal transition also has been detected in Si upon melting from the crystalline state.^{1,2} The structure of both systems is, however, more complicated than simple liquid metals.^{3,4} This intriguing property has motivated several studies of liquid Ge and Si from experimental and theoretical standpoints.

The structure of liquid Ge has been characterized by neutron-diffraction⁵ and x-ray² experiments, showing a low coordination number (between 5 and 7). Most liquid metals have almost a close-packed structure with a coordination number ~ 12 .³ These results have been interpreted by several authors as the persistence of covalent structures,¹ and moreover, by the existence of transient Ge clusters with fast exchange in the fluid phase.⁶ Self-diffusion studies in liquid Ge have shown that in the temperature range of 1200–1500 K there is an abrupt decrease in the diffusion coefficient as the melting point (T_M) is approached, indicating a rearrangement of the short-range order.⁷

Theoretical work on liquid Ge has been dedicated to studying its electronic and structural properties using various techniques. Linearized-muffin-tin orbital calculations predicted an electronic structure for liquid Ge far from the free-electron model and from any of the crystalline (semiconductor or metallic) phases.⁸ Density-functional theory⁹ and pseudopotential methods¹⁰ have been used to produce pair potentials which lead to structure factors and pair-correlation functions in agreement with experiments. Recently, an *ab initio* molecular-dynamics calculation of liquid Ge at 1250 K has appeared in the literature.¹¹ This work was based on conjugate-gradient techniques for energy minimization at each time step of the simulation, and in subspace alignment to predict the wave functions for new atomic positions. This approach was used to control adiabaticity in the metallic system. The pair-correlation function as well as the

electronic density of states were found in agreement with x-ray² and photoemission¹² experiments, respectively.

In this paper we present the results of an *ab initio* molecular-dynamics simulation of liquid Ge at 1500 K in which two Nosé thermostats are used. This is an alternative way to control adiabaticity, preventing the deviation of the electronic wave functions from the ground state during the coupling with ionic degrees of freedom. Our goal in performing this calculation is, in addition to obtaining structural and electronic information at higher temperatures, to study dynamical properties of liquid Ge. As it is well recognized, the *ab initio* molecular-dynamics method is an efficient scheme to generate from first principles the Born-Oppenheimer dynamics of the nuclei. In the present case, we analyze the effects of the interplay between the electronic structure and the atomic dynamics in liquid Ge. Of particular interest is determining if the covalent structures present in the fluid phase at 1270 K (Ref. 5) will survive at 1500 K.

In the following section we present a description of the method as well as computational details. Section III contains the results and a discussion. Finally, in Sec. IV we present the conclusions of this work.

II. THEORY

A. Method

We used the *ab initio* molecular-dynamics scheme, developed by Car and Parrinello.¹³ In this scheme the Kohn-Sham equations of the local-density-functional theory (LDF) (Ref. 14) are solved iteratively, treating the atomic coordinates $\{\mathbf{R}_I\}$ and the electronic wave functions $\{\psi_i\}$, corresponding to occupied states, as dynamical degrees of freedom of a fictitious classical system described by the following equations of motion:

$$\begin{aligned} \mu \ddot{\psi}_i(\mathbf{r}, t) &= -\frac{\delta E}{\delta \psi_i^*(\mathbf{r}, t)} + \sum_j \Lambda_{i,j} \psi_j(\mathbf{r}, t) \\ &= -H \psi_i(\mathbf{r}, t) + \sum_j \Lambda_{i,j} \psi_j(\mathbf{r}, t), \end{aligned} \quad (1)$$

$$M_I \ddot{\mathbf{R}}_I = -\nabla_{\mathbf{R}_I} E, \quad (2)$$

where the dots indicate time derivatives, M_I denotes atomic masses, μ is an adjustable parameter setting the time scale for the fictitious electronic dynamics, $\Lambda_{i,j}$ are Lagrange multipliers used to satisfy the orthonormality constraints on $\psi_i(\mathbf{R}, t)$, and $E[\{\psi_i\}, \{\mathbf{R}_I\}]$ is the LDF energy functional with the local-density approximation for exchange and correlation, plus the ionic Coulomb interaction.

$E[\{\psi_i\}, \{\mathbf{R}_I\}]$ acts as the potential energy of the fictitious system. If the Born-Oppenheimer (BO) approximation holds within the density-functional theory, the many-body potential $\Phi[\{\mathbf{R}_I\}]$ which defines the BO potential-energy surface for the ions, corresponds to the minimum of $E[\{\psi_i\}, \{\mathbf{R}_I\}]$ with respect to the ‘‘electronic degrees of freedom’’ $\{\psi_i\}$:

$$\Phi[\{\mathbf{R}_I\}] = \min_{\{\psi_i\}} E[\{\psi_i\}, \{\mathbf{R}_I\}]. \quad (3)$$

To solve Eqs. (1) and (2), the ground-state Kohn-Sham functions for $\{\mathbf{R}_I(t=0)\}$, with time derivatives $\dot{\psi}(t=0)$ equal to zero, are taken as initial conditions for the electronic degrees of freedom, i.e., E is initially equal to Φ . If the classical kinetic energy for the electronic degrees of freedom is much smaller than the ionic kinetic energy, the electrons are very close to the ground state, i.e., E is very close to Φ , and Eq. (2) describes physical atomic trajectories. A condition for the applicability of the Car-Parrinello method is that the time scale for the heat transfer from the ions to the electrons is so long that no deviations from the BO surface occurs during the molecular-dynamics (MD) simulation time. This can be achieved for the case of insulators by an appropriate choice of μ . For the case of metallic systems, energy transfer on a relatively small time scale occurs for any choice of μ . This problem can be circumvented by introducing two Nose¹⁵ thermostats, having masses Q_R and Q_e , associated with the ions and electrons, respectively.¹⁶ The ionic thermostat is used to keep the average ionic temperature equal to the preset value T , while the electronic thermostat is used to keep the total classical kinetic energy of the electronic degrees of freedom very close to a preset value $E_{\text{kin},0}$. The equations of motion can be now written as

$$M_I \ddot{\mathbf{R}}_I = -\nabla_{\mathbf{R}_I} E - M_I \dot{\mathbf{R}}_I \dot{x}_R, \quad (4)$$

$$Q_R \ddot{x}_R = 2 \left(\sum_I \frac{1}{2} M_I \dot{\mathbf{R}}_I^2 - \frac{1}{2} g k_B T \right), \quad (5)$$

$$Q_e \ddot{x}_e = 2(\mu \langle \dot{\psi} | \dot{\psi} \rangle - E_{\text{kin},0}), \quad (6)$$

where x_e and x_R are the thermostat degrees of freedom.

B. Computational details

We have used a cubic cell containing 64 atoms with periodic boundary conditions of the simple cubic type. The cell size is chosen as 11.196 Å, giving the experimental number density at $T \sim T_M$, $n = 0.0456 \text{Å}^{-3}$.¹⁷ The electronic wave functions are expanded in plane waves with a kinetic-energy cutoff of 12 Ry. Only the Γ point was used to sample the Brillouin zone of the molecular-dynamics (MD) supercell. The norm-conserving pseudopotential is taken from Ref. 18, and includes both s and p nonlocal terms, which are treated within the Kleinman-Bylander scheme.¹⁹ This pseudopotential has been used extensively in the study of bulk Ge,²⁰ and the (111) surfaces of Ge, both at $T = 0$ K (Ref. 21) and at finite temperatures,²² giving excellent results.

To prepare the liquid, the atoms are initially arranged in the diamond structure. They are given random displacements corresponding to $T \sim 300$ K. Then the temperature is raised gradually up to 2000 K, well above the melting point. The system is kept at this temperature until the mean square displacement shows diffusive behavior typical of a liquid. The temperature is then reduced to ~ 1500 K, above the experimental melting point of 1250 K. The system is equilibrated for a few thousand time steps (the integration time step was 2.4×10^{-16} s), and statistics are collected for around 2.4 ps.

III. RESULTS AND DISCUSSION

A. Structural properties

Using the ionic coordinates of the configurations collected during the last 2.4 ps of the simulation, we obtained the static structure factor $S(k)$ and the pair-correlation function $g(r)$, and show them in Figs. 1(a) and 1(b), respectively, together with x ray² and neutron-scattering⁵ data. Considering the differences between the two sets of experimental data, the agreement of our results is excellent. The first peak of $S(k)$ is asymmetric, with a shoulder on the high- k side. This shoulder has been interpreted as coming from covalent bonds that remain in the liquid. The first peak in $g(r)$ is also asymmetric, and there is a hump between the first peak positioned at 2.63 Å and the second one at 5.72 Å. This hump was considered as a characteristic feature of $g(r)$ for tetravalent elements by Hafner and Kahl.⁴ In the present case, as in the neutron-scattering data the hump is not as sharp as in the x-ray-diffraction data and in the calculation of Kresse and Hafner.¹¹ The average coordination number, as obtained by integrating $g(r)$ up to the first minimum $r_m = 3.35$ Å is ~ 7.0 in close agreement with the x-ray experimental values of 6.8 (Ref. 3), and 7.1.²³ It is somewhat higher than the value found by Kresse and Hafner of 6.2.¹¹ This is not surprising since we are using higher density and temperature. In Fig. 2 it can be seen that there is a broad distribution of local coordination numbers dominated by the sixfold and sevenfold. In the case of liquid Si,²⁴ this distribution is centered at the sixfold, indicating a lower local coordination. Additional information on the short-range order can be obtained

from higher-order correlation functions, in particular, the triplet correlation function. This is especially important in our case since the system retains some covalent bonding effects and has directional forces. Triplet correlations are expressed in terms of the bond angles between the two vectors that join a central atom with two neighbors at a distance less than r_m . Figure 3 shows that short bonds form angles broadly distributed around the tetrahedral angle, while longer bonds form angles distributed around $\theta \sim 60^\circ$ and $\sim 90^\circ$. These results are similar to those found in liquid Si,²⁴ and to the results of Kresse and Hafner.¹¹ However for the case of large bonds, e.g., $R_m = 3.3 \text{ \AA}$, our peak close to $\theta \sim 60^\circ$ is not as sharp as the one of Kresse and Hafner.¹¹ Again, we interpret this difference as coming from the higher temperature and/or density we are using in the present calculation.

B. Dynamical properties

The atomic trajectories of our MD simulation allow us to study time-dependent phenomena and transport properties. The diffusion coefficient D can be evaluated

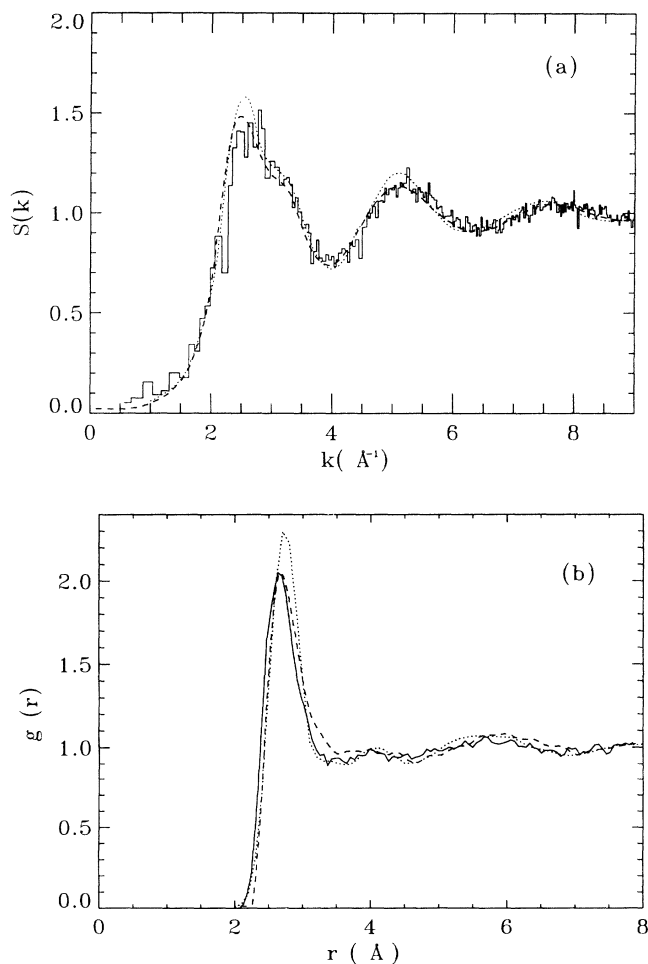


FIG. 1. (a) Structure factor $S(k)$, and (b) radial distribution function $g(r)$ of liquid Ge. Solid line, this calculation; dashed line, neutron scattering experiment (Ref. 5); dotted line, x-ray experiment (Ref. 2).

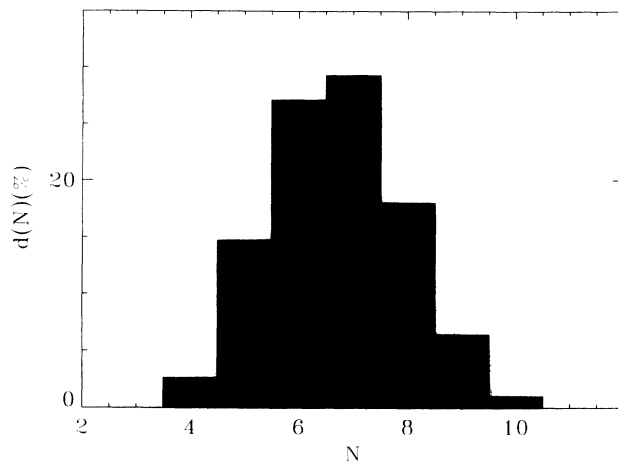


FIG. 2. Distribution $d(N)$ of local coordination numbers in liquid Ge. The coordination shell is obtained by counting the number of atoms at a distance shorter than r_{\min} , the first minimum in $g(r)$.

from the behavior of the mean square displacement $\mathbf{R}^2(t)$ for large t , using the Einstein relation²⁵

$$\mathbf{R}^2(t) \equiv \frac{1}{N} \sum_{I=1}^N [\mathbf{R}_I(t) - \mathbf{R}_I(0)]^2 = 6Dt. \quad (7)$$

A quasilinear behavior in the mean square displacement along the entire simulation time of 2.4 ps, characteristic of a diffusive motion, is shown in Fig. 4. A least-squares fit gives a value of $D \sim 1.2 \times 10^{-4} \text{ cm}^2 \text{ s}^{-1}$. Close to the melting point, Pavlov and Dobrokhotov⁷ reported two self-diffusion coefficients: one of $D \sim 1.21 \times 10^{-4} \text{ cm}^2 \text{ s}^{-1}$ (similar to the value found in the present study), and the other of $0.78 \times 10^{-4} \text{ cm}^2 \text{ s}^{-1}$. In the range of 1350–1500 K, their values vary from $1.62 \times 10^{-4} \text{ cm}^2 \text{ s}^{-1}$ up to $3.21 \times 10^{-4} \text{ cm}^2 \text{ s}^{-1}$. We remark here that although our simulated sample shows good liquidlike behavior, we do

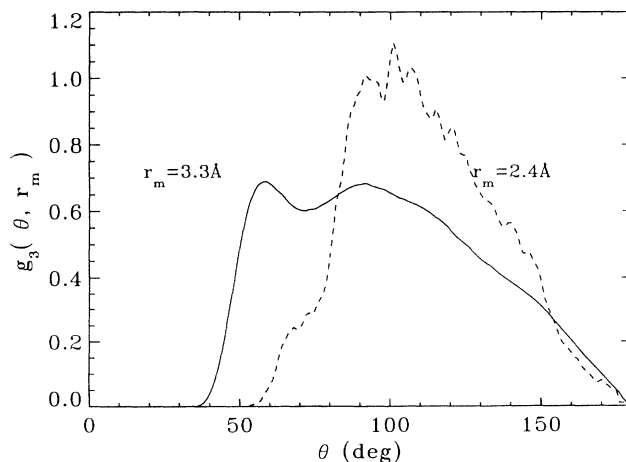


FIG. 3. Bond-angle distribution function $g_3(\theta, r_m)$ for liquid Ge at $T \sim 1500 \text{ K}$ calculated for different values of the maximum bond length r_m . The full line is obtained by taking r_m equal to the first minimum in $g(r)$. The dashed line was obtained using the bond length of crystalline Ge.

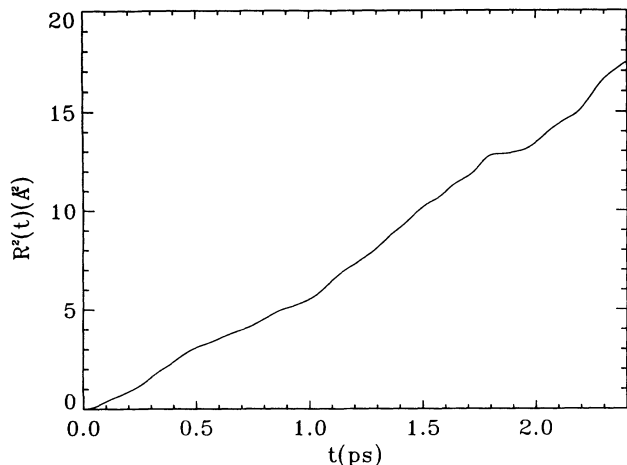


FIG. 4. Mean square displacement $R^2(t)$ as a function of time in liquid Ge at $T \sim 1500$ K.

not know the precise value of its melting point. Considering this fact, and also the strong dispersion of the experimental data in the whole temperature range, especially around the melting point, we find our diffusion coefficient to be in satisfactory agreement with these experimental results. Our value is also consistent with the one obtained for liquid Si (Ref. 24) ($D \sim 2.26 \times 10^{-4} \text{ cm}^2 \text{ s}^{-1}$ at $T = 1800$ K), since the mass effect is higher in liquid Ge. From Fig. 4 we observe that on average each Ge atom has traveled a distance of $\sim 2.1 \text{ \AA}$ in 1 ps while during the same time a Si atom has diffused by $\sim 3.7 \text{ \AA}$.²⁴ Along the total time of the simulation a Ge atom has moved by $\sim 5.1 \text{ \AA}$, close to one crystal lattice constant.

Additional information on the dynamical behavior of liquid Ge can be obtained from the power spectrum $I(\nu)$, the Fourier transform of the velocity autocorrelation function $C(t)$,

$$I(\nu) = 2 \int_0^\infty C(t) \cos 2\pi\nu t dt, \quad (8)$$

where $C(t)$ is defined as

$$C(t) = \frac{\langle \mathbf{v}(0) \cdot \mathbf{v}(t) \rangle}{\langle \mathbf{v}(0) \cdot \mathbf{v}(0) \rangle}. \quad (9)$$

In Fig. 5 we plot $I(\nu)$ using two different correlation times: $t = 0.7$ ps for the solid line and $t = 1.1$ ps for the dashed line. In agreement with tight-binding molecular-dynamics calculations for *l*-Si,²⁶ we observe that the features present in $I(\nu)$ become more pronounced as the correlation time is increased. For both cases, in addition to the diffusive modes at low frequencies, it is notorious the presence of bumps at intermediate frequencies which can be associated to vibrational modes coming from the covalent bonds still present in the liquid. A similar situation has been found by Štich *et al.*²⁴ for liquid Si. They obtained a shoulder in $I(\nu)$ in the frequency range of 9–10 THz which was interpreted as a reminiscence of the vibrational motion of covalent bonds. The bumps observed in liquid Ge around 4 THz are consistent with the feature

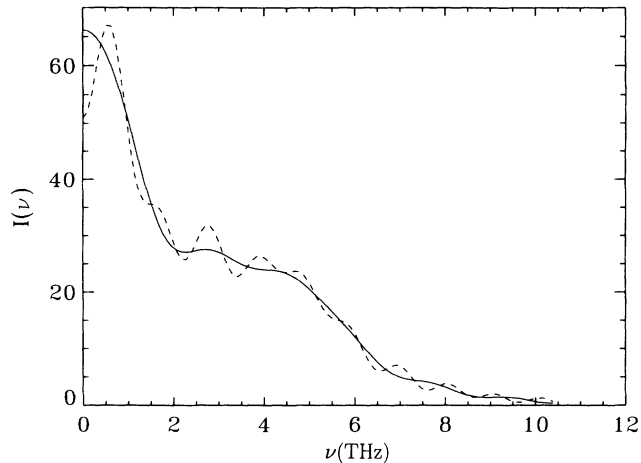


FIG. 5. Power spectrum $I(\nu)$ as a function of frequency in liquid Ge at $T \sim 1500$ K for two different times: (a) $t = 0.7$ ps for the solid line, and (b) $t = 1.1$ ps for the dashed line.

observed in liquid Si, given the mass difference between these elements.

C. Bonding and electronic properties

The low coordination number in liquid Ge compared with the one seen in simpler liquid metals suggests that covalent bonds similar to those of crystalline Ge may still be present in the liquid. This idea was proposed by Ascroft,⁶ to explain the shoulder observed in the first peak of the structure factor $S(k)$.⁵ To investigate this question further, we have performed an analysis of the charge distribution which in the *ab initio* MD scheme is generated together with the atomic trajectories. In Fig. 6, we compare bonding characteristics in crystalline Ge, and temporal bond sites in a typical configuration of liquid Ge (taken at the end of the simulation time). We can clearly see from these plots the presence of covalent bonds between three of the atoms in the liquid. In Fig. 6(b) the two neighbors of the central atom are at distances close to those of crystalline Ge, and the angle

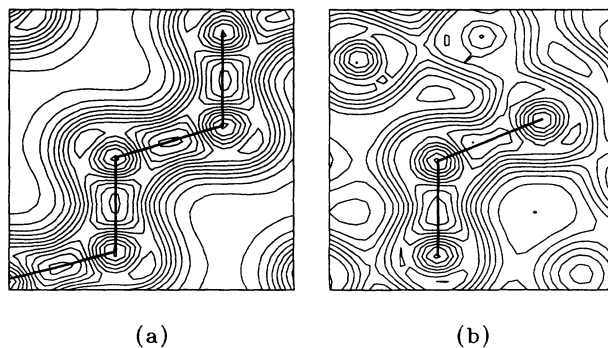


FIG. 6. Contour plots of the valence-electronic charge density. (a) Crystalline Ge in the (110) plane. (b) A typical configuration of liquid Ge in the plane formed by the three atoms joined by bonds.

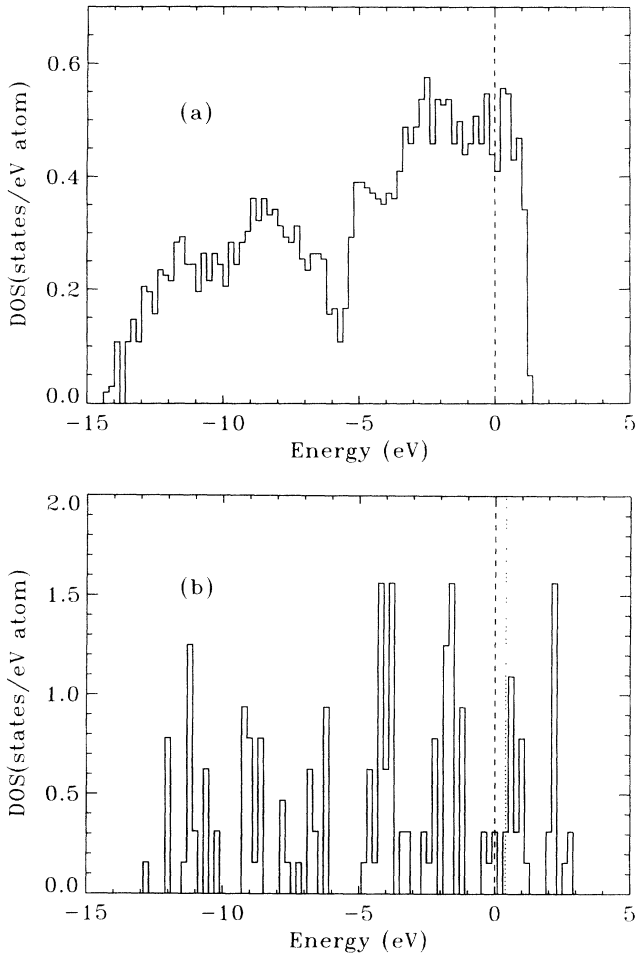


FIG. 7. Density of states $DOS(E)$ of (a) liquid Ge at $T \sim 1500$ K, and (b) bulk Ge at $T = 0$ K. The dashed line corresponds to the highest occupied state and the dotted line to the lowest unoccupied state. The energy gap for the bulk case is 0.4 eV.

formed by their bonds is very similar to the tetrahedral angle, characteristic of sp^3 hybridization.

To see if the formation of temporal covalent bonds affect the metallicity of liquid Ge we calculated the electronic density of states by averaging over 16 different

ionic configurations. The lowest 160 Kohn-Sham states at the Γ point are used for each set of R_I [Fig. 7(a)]. They are calculated using a conjugate-gradient minimization procedure. For comparison we show in Fig. 7(b) the density of states of bulk Ge at $T = 0$ K, calculated using our 64-atom supercell, and the same energy cutoff of 12 Ry. We found an energy gap of 0.4 eV. From Fig. 7(a) it can be clearly seen that *l*-Ge is metallic, with a deep pseudogap about 5 eV below the Fermi level. This density of states is in good agreement with experimental results²⁷ and other theoretical calculations.¹¹ The pseudogap is characteristic of heavier elements but not of Si, which is more free-electron-like. Jank and Hafner⁸ have shown that the formation of the pseudogap is due to a *s-p* splitting arising from relativistic effects that are more important in heavier elements like Ge.

IV. CONCLUSIONS

The *ab initio* molecular-dynamics method was used to study structural, dynamical, and electronic properties of liquid Ge at $T = 1500$ K. Two Nosé thermostats were coupled to the system to control adiabaticity and avoid the instabilities in the metallic liquid Ge. Good agreement with available experiments and other theoretical calculations was obtained. In particular, the structural and electronic properties are similar to those obtained by Kresse and Hafner¹¹ using an alternative method to preserve adiabaticity. The dynamical behavior of liquid Ge at 1500 K shows the persistence of some covalent bonds in the melt. The calculated diffusion coefficient is in satisfactory agreement with available experimental data. In a system like this, where covalent and metallic behavior coexist, it is important to incorporate the interplay between electronic structure and atomic motion, that only *ab initio* molecular dynamics can provide.

ACKNOWLEDGMENTS

This work was supported by the Supercomputing Center DGSCA-UNAM, DGAPA-UNAM Project IN107294IF, and by CONACYT Project No. D111-904360. N.T. acknowledges financial support from CONACYT. We thank A. Selloni for valuable comments and A. Reyes for technical support.

¹V.M. Glazov, S.N. Chizhevskaya, N.N. Glagoleva, *Liquid Semiconductors* (Plenum, New York, 1969).

²Y. Waseda, *The Structure of Non-Crystalline Materials; Liquids and Amorphous Solids* (McGraw-Hill, New York, 1980).

³Y. Waseda and K. Susuki, *Z. Phys. B* **20**, 339 (1975).

⁴J. Hafner and G. Kahl, *J. Phys. F* **14**, 2259 (1984).

⁵P.S. Salmon, *J. Phys. F* **18**, 2345 (1988).

⁶N.W. Ashcroft, *Nuovo Cimento D* **12**, 597 (1990).

⁷P.V. Pavlov and E.V. Dobrokhotov, *Fiz. Tverd. Tela (Leningrad)* **12**, 281 (1970) [*Sov. Phys. Solid State* **12**, 225 (1970)].

⁸W. Jank and J. Hafner, *Europhys. Lett.* **7**, 623 (1988).

⁹M.W.C. Dharma-wardana and F. Perrot, *Phys. Rev. Lett.* **65**, 76 (1990).

¹⁰A. Arnold, N. Mauser, and J. Hafner, *J. Phys. Condens. Matter* **1**, 965 (1989).

¹¹G. Kresse and J. Hafner, *Phys. Rev. B* **47**, 558 (1993).

¹²G. Indlekofer, P. Oelhafen, R. Lapka, and H.J. Güntherodt, *Z. Phys. Chem.* **157**, 465 (1988).

¹³R. Car and M. Parrinello, *Phys. Rev. Lett.* **55**, 2471 (1985).

¹⁴W. Kohn and L.J. Sham, *Phys. Rev.* **140**, A1133 (1965).

¹⁵S. Nosé, *Mol. Phys.* **52**, 255 (1984); *J. Chem. Phys.* **81**, 511 (1984).

¹⁶P.E. Blöchl, and M. Parrinello, *Phys. Rev. B* **45**, 9413 (1992).

¹⁷*CRC Handbook of Chemistry and Physics*, 67th ed., edited by R.C. Weast (CRC, Boca Raton, FL, 1987).

¹⁸R. Stumpf, X. Gonze, and M. Scheffler (unpublished).

¹⁹L. Kleinman and D. M. Bylander, *Phys. Rev. Lett.* **48**, 1425

- (1982).
- ²⁰A.I. Shkrebtii *et al.* (unpublished).
- ²¹N. Takeuchi, A. Selloni, A.I. Shkrebtii, and E. Tosatti, *Phys. Rev. B* **44**, 13 611 (1991); N. Takeuchi, A. Selloni, and E. Tosatti, *Phys. Rev. Lett.* **69**, 648 (1992).
- ²²N. Takeuchi, A. Selloni, and E. Tosatti, *Phys. Rev. B* **49**, 10 757 (1994); *Phys. Rev. Lett.* **72**, 227 (1994).
- ²³S.P. Isherwood, B.R. Orton, and R. Mänälä, *J. Non-Cryst. Solids* **8-10**, 691 (1972); B.R. Orton and S.P. Woodisse, *J. Phys. F* **3**, 1141 (1973).
- ²⁴I. Štich, R. Car, and M. Parrinello, *Phys. Rev. B* **44**, 4262 (1991).
- ²⁵D. Chandler, *Introduction to Modern Statistical Mechanics* (Oxford University Press, New York, 1987).
- ²⁶E. Kim, and Y. H. Lee, *Phys. Rev. B* **49**, 1743 (1994)
- ²⁷M.K. Gardiner, D. Colbourne, and C. Norris, *Philos. Mag. B* **54**, 133 (1986).

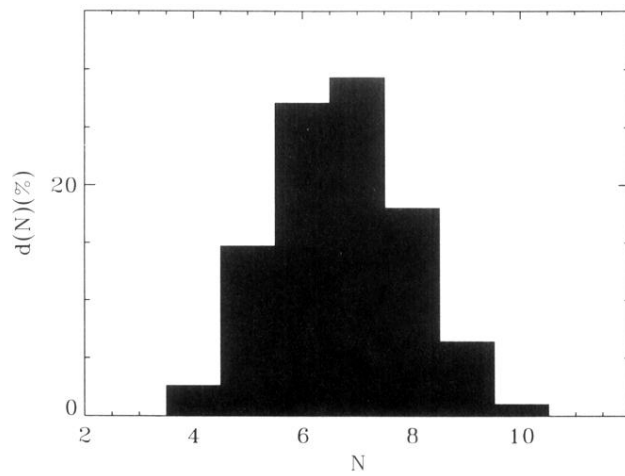


FIG. 2. Distribution $d(N)$ of local coordination numbers in liquid Ge. The coordination shell is obtained by counting the number of atoms at a distance shorter than r_{\min} , the first minimum in $g(r)$.